MAX PLANCK INSTITUTE
FOR DYNAMICS OF COMPLEX
TECHNICAL SYSTEMS
MAGDEBURG

25
1998
2023

CSC
COMPUTATIONAL METHODS IN
SYSTEMS AND CONTROL THEORY

Infering Discrete and Reduced Fluid-Structure Interaction Models from Data

Leonidas Gkimisis, Süleyman Yıldız, Thomas Richter,
Peter Benner

Trends in Scientific Computing - 30 Jahre Wissenschaftliches Rechnen in Dortmund
TU Dortmund, May 21-22, 2024

Overview

- **Adjacency-based non-intrusive modelling**
  - Inference of Numerical Schemes
  - Motivating example: 2D Burgers' equation

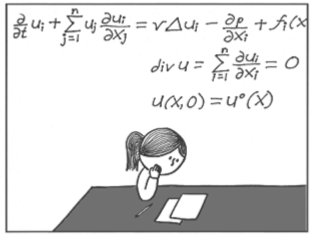

- **Application to incompressible Navier Stokes**
  - Inference of sparse FOM / POD
  - Numerical Aspects (centering / regularization)
  - sFOM-POD / OpInf comparison (cylinder flow)

- **Fluid-Structure Interactions (FSI)**
  - Governing Equations
  - Laminar Vortex-Induced Vibrations (VIV)
  - Hron-**Turek** Benchmark FSI3

Inference of Numerical Schemes

- We look at PDEs of the form: $\frac{\partial u}{\partial t} = \mathcal{P}(u, u_x, u_{xx}, u_y, u_{yy}, u_{xy}..)$, where $\mathcal{P}(.)$ is a polynomial operator.

- Discretizing the right hand side in space, we obtain a system of ODEs for each spatial point $\vec{x}_i$:

$$\left.\frac{du}{dt}\right|_{\vec{x}_i} = \sum_{j \in q_i} f_j \beta_j = \mathbf{f}_{q_i}^T \boldsymbol{\beta}_i$$

e.g. for a 1D linear system *(heat eq.)* and a 3-pt symmetric stencil:

$$\mathbf{f}_{q_i} = [u_{i-1}, u_i, u_{i+1}]^T$$

and $\boldsymbol{\beta}_i$ are corresponding coefficients.

Numerical Scheme Inference: Can we infer $\boldsymbol{\beta}_i$, given data over $t \in [t_1, t_N]$ for $\left.\frac{du}{dt}\right|_{\vec{x}_i}$ and $\mathbf{f}_{q_i}$?

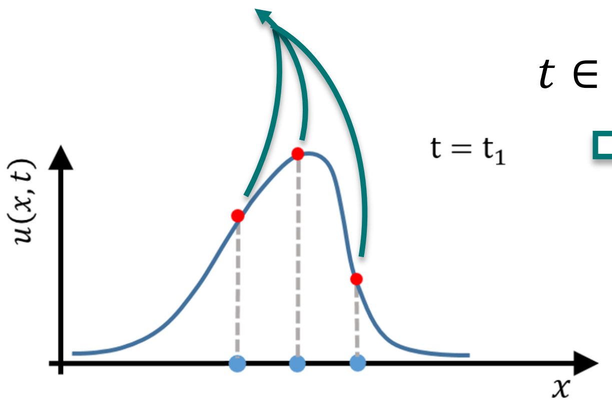

$t \in [t_1, t_N]$

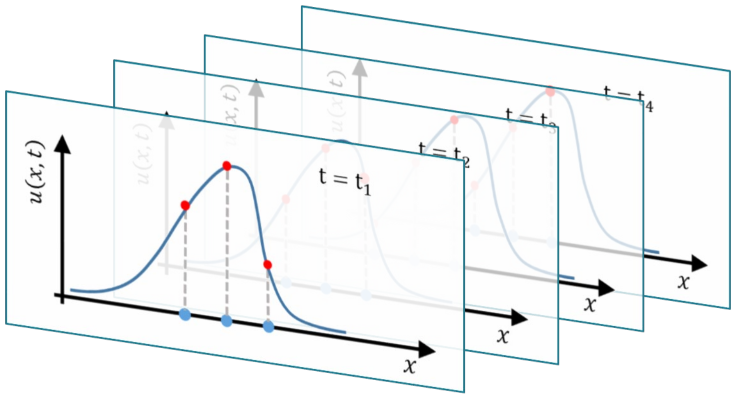

...

Least squares formulation:

$$\min_{\boldsymbol{\beta}_i} \|\mathcal{D}_i \boldsymbol{\beta}_i - \mathbf{d}_i\|_2$$

with: $\mathcal{D}_i = \begin{bmatrix} \mathbf{f}_{q_i}^T(t_1) \\ \vdots \\ \mathbf{f}_{q_i}^T(t_N) \end{bmatrix}$, $\mathbf{d}_i = \begin{bmatrix} \left.\frac{du}{dt}\right|_{(i,t_1)} \\ \vdots \\ \left.\frac{du}{dt}\right|_{(i,t_N)} \end{bmatrix}$

Baddoo et al. (2021), Schumann Y., & Neumann P. (2022)

A nonlinear example: 2D Burgers' equation

$$\frac{\partial u}{\partial t} = cu\nabla \cdot u + \nu \nabla^2 u$$

Periodic BCs for $(x, y) \in [0,1] \times [0,1]$

$$u(t=0) = cos(2\pi x)cos(2\pi y)$$

Discretizing in space and time, we get:

$$\mathbf{u}_{n+1} = A\mathbf{u}_n + Q\mathbf{u}_n \circ \mathbf{u}_n$$

where A and Q are sparse matrices.

We aim to infer the entries of A, Q. These correspond to vector $\boldsymbol{\beta}_\alpha$

$$\min_{\boldsymbol{\beta}_\alpha} \|\mathcal{D}_\alpha \boldsymbol{\beta}_\alpha - \mathbf{d}_\alpha\|_2$$

Numerical stencil:

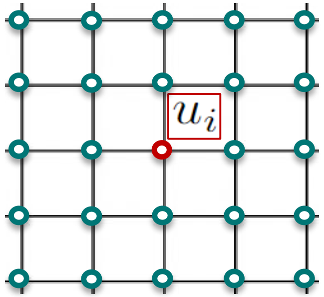

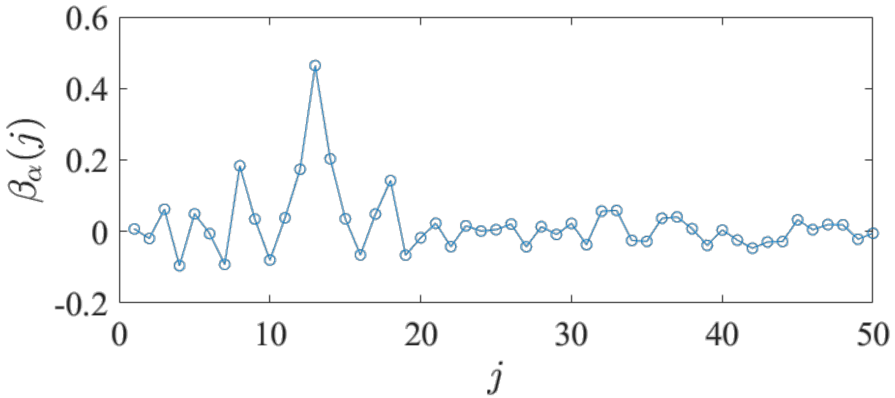

- We collect data for $\nu = 2 \times 10^{-3}, c = 0.2, \Delta x = \Delta y = 0.02, \Delta t = 0.01$, using a second-order scheme in space.
- Regularization is necessary: We truncate the SVD of $\mathcal{D}_\alpha$, which is equivalent to an L_2 regularization:

$$\min_{\boldsymbol{\beta}_\alpha} \|\mathcal{D}_\alpha \boldsymbol{\beta}_\alpha - \mathbf{d}_\alpha\|_2^2 + \lambda \|\boldsymbol{\beta}_\alpha\|_2^2$$

- Observation: A strict truncation limit of $\sigma / \max(\sigma) = 10^{-4}$ is needed: Potentially linked to the order of the scheme used for simulation.

A nonlinear example: 2D Burgers'

Simulation results:

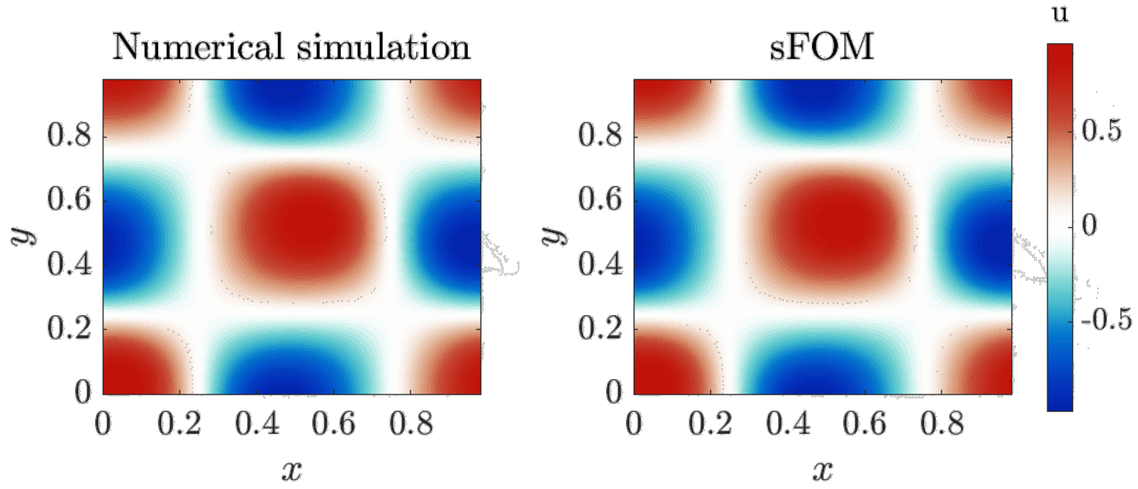

We simulate the inferred system with different initial conditions: $u(t=0) = e^{-10(x-0.5)^2} e^{-10(y-0.5)^2}$

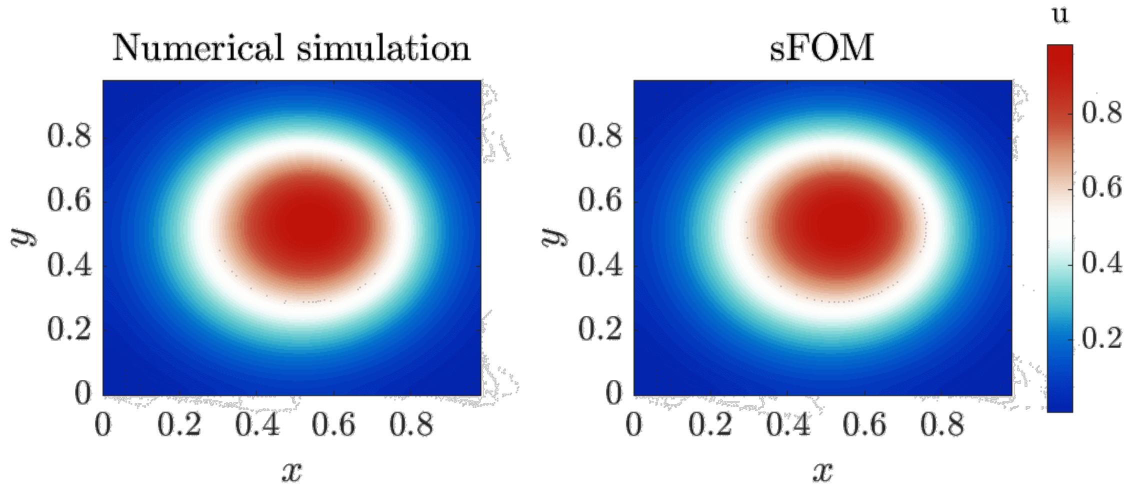

Sparse FOM for incompressible N-S

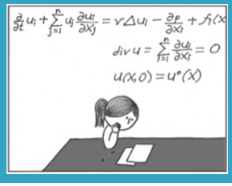

Incompressible N-S:

$$\begin{cases} \nabla \cdot \mathbf{u} = 0 \\ \dfrac{\partial \mathbf{u}}{\partial t} + (\mathbf{u} \cdot \nabla)\mathbf{u} = \dfrac{1}{\rho_f} \nabla \cdot \sigma + \mathbf{f} \end{cases}$$

Discretizing in space:

$$\begin{cases} \dfrac{\partial \mathbf{u}}{\partial t} = A_1 \mathbf{u} + A_2 \mathbf{p} + H \mathbf{u} \otimes \mathbf{u} \\ A_2^T \mathbf{u} = \mathbf{0} \end{cases}$$

where: $A_1 \in \mathcal{R}^{n_u \times n_u}$, $A_2 \in \mathcal{R}^{n_u \times n_p}$, $H \in \mathcal{R}^{n_u \times n_u^2}$

In projection-based methods:

$$\tilde{\mathbf{u}} = U^T \mathbf{u}$$

where $U \in \mathcal{R}^{n_u \times r}$
and $r \ll n_u$

...after cancelling out pressure:

$$\mathbf{u}^{k+1} = \mathbf{A}\,\mathbf{u}^{k} + \mathbf{H}\,\mathbf{u}^{k} \otimes \mathbf{u}^{k} + \mathbf{K}\,\mathbf{u}_{in} + \mathbf{C}$$

P.B. et al. (2021)

with adjacency-based, sparse **A, H, K**

We can use the local inference of numerical schemes, scaling with n_u

Pros:

(+) Direct enforcement of Dirichlet BCs (e.g. **K** known a priori).
(+) FOM independence from projection basis.

Cons:

(-) ↑↑ in offline computational cost.
(-) Need for adjacency information (mesh construction).

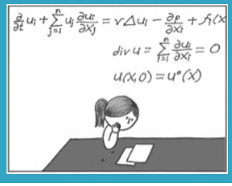

Sparse FOM inference - POD

1st step: Interpolate data ∀t to a grid (or construct adjacency matrix of an existing grid).

2nd step: To enforce adjacency-based sparsity, we examine each DOF i independently:

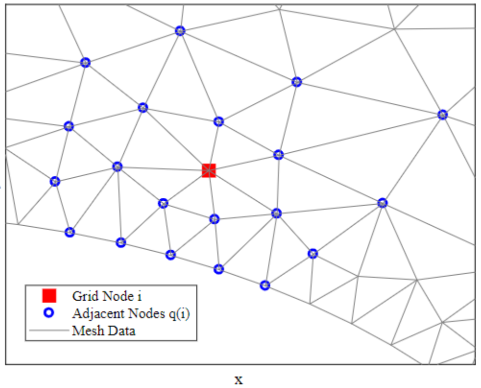

adj. info +
data for t ∈ $[t_1, t_N]$

Least-Squares formulation

$$\min_{\beta_i} \|\mathcal{D}_i \beta_i - \mathbf{d}_i\|_2^2 + \lambda_i \|\beta_i\|_2^2$$

where:

$$\mathcal{D}_i = \begin{bmatrix} \mathbf{f}_{q_i}^T(t_1) \\ \vdots \\ \mathbf{f}_{q_i}^T(t_N) \end{bmatrix}, \quad \mathbf{d}_i = \begin{bmatrix} \frac{du}{dt}\big|_{(i,t_1)} \\ \vdots \\ \frac{du}{dt}\big|_{(i,t_N)} \end{bmatrix}$$

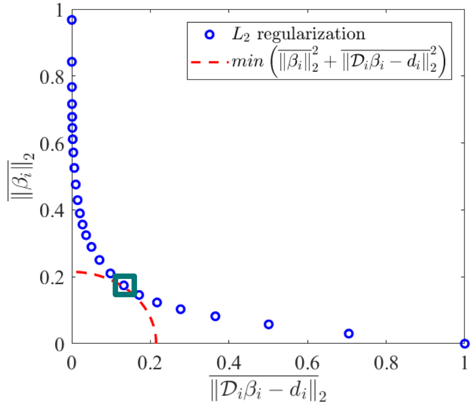

Interpolating over (x, y): λ_i

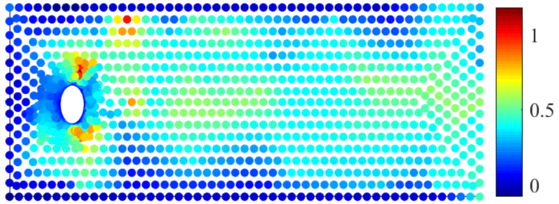

3rd step: Store the values of β_i to the FOM sparse matrices.

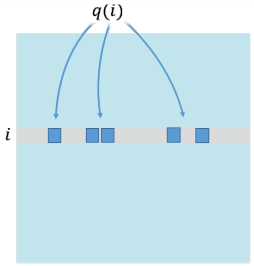

"smart" projection due to known sparsity

4th step: Project to ROM through Proper Orthogonal Decomposition (POD). e.g: $\tilde{A} = U^T A U$ $\tilde{H} = U^T H U \otimes U$

Cylinder flow results

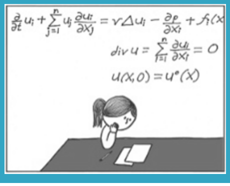

We examine this formulation for a laminar, incompressible flow over a cylinder:

- 65% training time for ROMs (over which system operators are inferred, also for OpInf (Peherstorfer, & Willcox (2016)).
- Average error over the domain: $e(t) = \frac{\|\mathbf{u}_{x_{CFD}} - \mathbf{u}_{x_{ROM}}\|_1}{n \max(\mathbf{u}_{x_{CFD}} - \overline{\mathbf{u}}_{x_{CFD}})} \times 100\%$

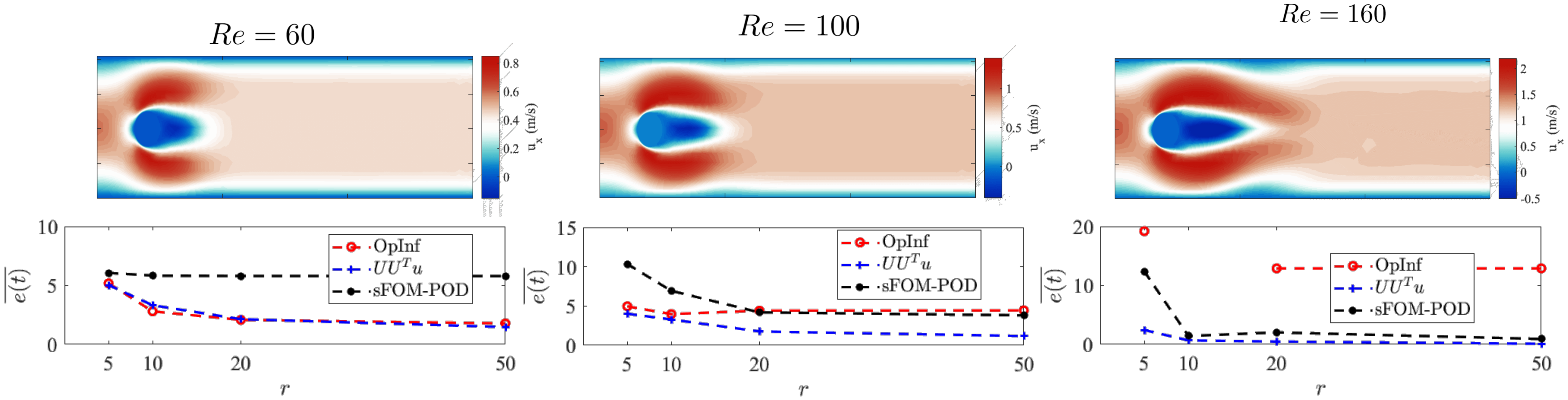

Computational (clock) offline time:
OpInf $O(t_{OpInf}) = 1\ s$, sFOM $O(t_{sFOM}) = 60\ s$

Numerical simulations performed with Gascoigne3D (open-source, finite element solver)

Fluid-Structure Interactions (FSI)

Incompressible N-S equations (Arbitrary Lagrangian-Eulerian formulation):

$$\begin{cases} \rho_f \left(\partial_t \hat{\mathbf{u}} + \hat{\nabla} \hat{\mathbf{u}} \;\; I \;\; \left(\hat{\mathbf{u}} - \partial_t \hat{\mathbf{d}} \right) \right) - \\ - \operatorname{div} \left(\;\; \hat{\sigma} \left(\hat{\mathbf{u}}, \hat{p} \right) \;\; I \;\; \right) = \;\; \rho_f \vec{g} \\ \operatorname{div} \left(\;\; I \;\; \hat{\mathbf{u}} \right) = 0 \end{cases}$$

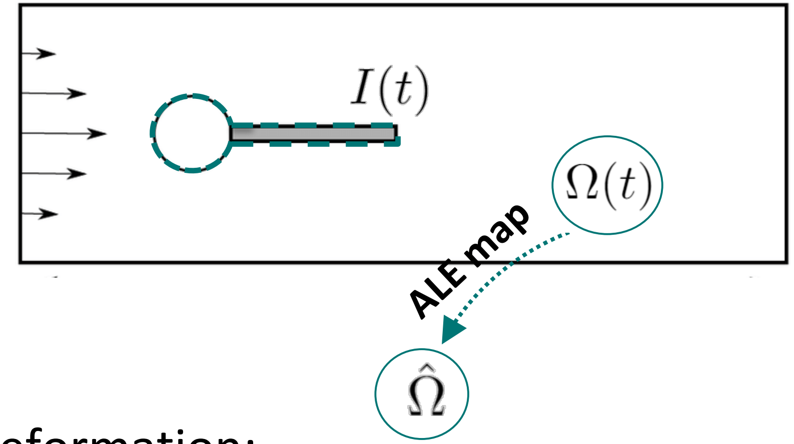

Solid Navier-Lamé equations:

$$\begin{cases} \partial_{tt} \mathbf{d}_s - \nabla \cdot \boldsymbol{\sigma}_s = 0 \\ \boldsymbol{\sigma}_s = \mu (\nabla \mathbf{d}_s + \nabla \mathbf{d}_s^T) + \lambda \, tr (\tfrac{1}{2} (\nabla \mathbf{d}_s + \nabla \mathbf{d}_s^T)) I \end{cases}$$

Grid deformation:

$$\begin{cases} -\nabla^2 \hat{\mathbf{d}}_f - \dfrac{\nabla a}{a} \nabla \hat{\mathbf{d}}_f = \mathbf{0}, & \text{in } \hat{\Omega} \times (0, T] \\ \hat{\mathbf{d}}_f = \hat{\mathbf{d}}_s - \hat{\mathbf{d}}_s (t = 0), & \text{on } I(t) \\ \hat{\mathbf{d}}_f = \mathbf{0}, & \text{on external boundaries} \end{cases}$$

Coupling conditions:

$$\begin{cases} \mathbf{n}_f \cdot \boldsymbol{\sigma}_f = -\mathbf{n}_s \cdot \boldsymbol{\sigma}_s \text{ on } \; I(t) \\ \partial_t \mathbf{d}_s = \mathbf{u}_f \text{ on } \; I(t) \end{cases}$$

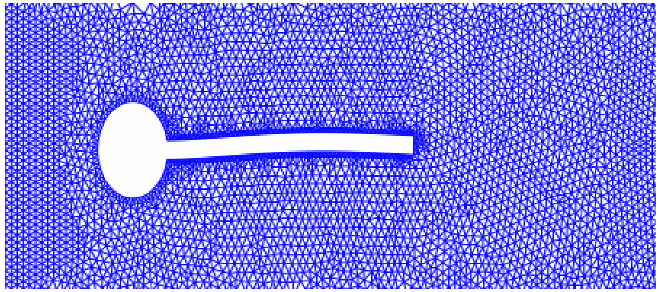

VIV: Coupled sFOM-POD/ First-principle models

Non-deformable solid dynamics (4 DOFs):

$$\rho_s A_s \partial_{tt}\mathbf{d}_s + K\mathbf{d}_s = (\rho_s - \rho_f)A_s\vec{g} + \int_{\partial S}\sigma(\mathbf{u},p)\vec{n}\,\mathrm{d}s$$

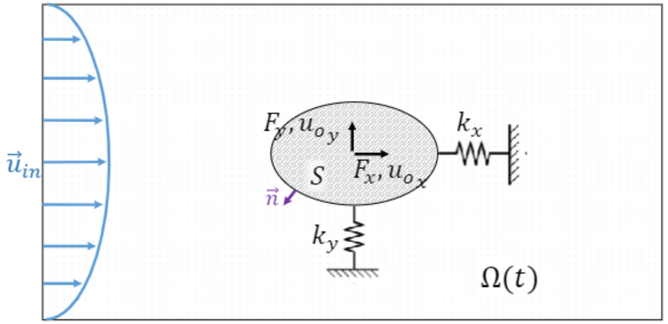

Quadratic-bilinear data-driven model for the fluid part:

$$\mathbf{u}_F^k = A\mathbf{u}_F^{k-1} + H\mathbf{u}_F^k \otimes \mathbf{u}_F^k + K\,\partial_t\mathbf{d}_s^k \otimes \mathbf{u}_F^k + B\,\partial_t\mathbf{d}_s^k + L\,\mathbf{u}_{in}^k + C_F$$

Performing POD, we obtain the coupled Fluid/Structure ROM:

Fluid part (data-driven)

$$\begin{cases} \tilde{\mathbf{u}}^k = \tilde{A}\tilde{\mathbf{u}}^{k-1} + \tilde{H}\tilde{\mathbf{u}}^k \otimes \tilde{\mathbf{u}}^k + \tilde{K}\partial_t\mathbf{d_s}^k \otimes \tilde{\mathbf{u}}^k + \\ \qquad + \tilde{B}\partial_t\mathbf{d_s}^k + \tilde{L}\mathbf{u}_{in} + \tilde{C} \\ \mathbf{F}^k = \tilde{A}_F\tilde{\mathbf{u}}^k + \tilde{H}_F\tilde{\mathbf{u}}^k \otimes \tilde{\mathbf{u}}^k \end{cases}$$

Solid part (physics)

$$\begin{cases} \partial_t\mathbf{d_s}^k + \frac{\Delta t K}{2\rho_s A_s}\mathbf{d_s}^k - \frac{\Delta t}{2}\mathbf{F}^k \\ = \partial_t\mathbf{d_s}^{k-1} - \frac{\Delta t K}{2\rho_s A_s}\mathbf{d_s}^{k-1} + \Delta t\,\mathbf{g} + \frac{\Delta t}{2}\mathbf{F}^{k-1} \\ \mathbf{d_s}^k - \frac{\Delta t}{2}\partial_t\mathbf{d_s}^k \\ = \mathbf{d_s}^{k-1} + \frac{\Delta t}{2}\partial_t\mathbf{d_s}^{k-1} \end{cases}$$

Results for $Re = 180$

ROM with 20 DOFs built for CFD data $t < 3.80\ s$, predictions for $t = 3.80 \rightarrow 5.91\ s$

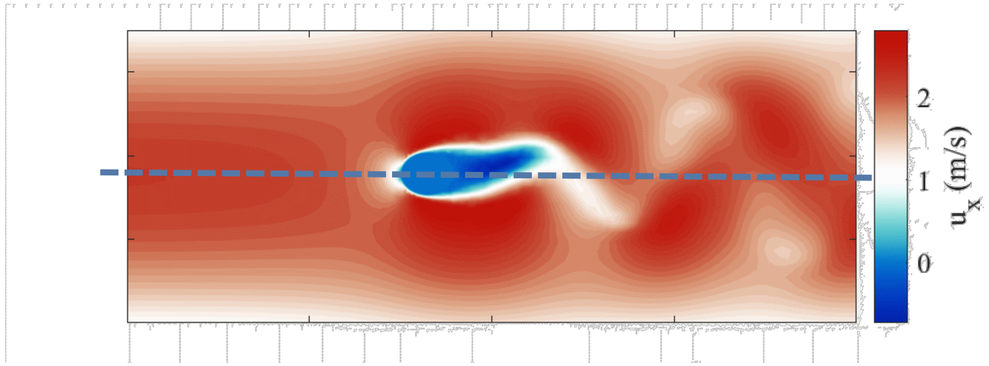

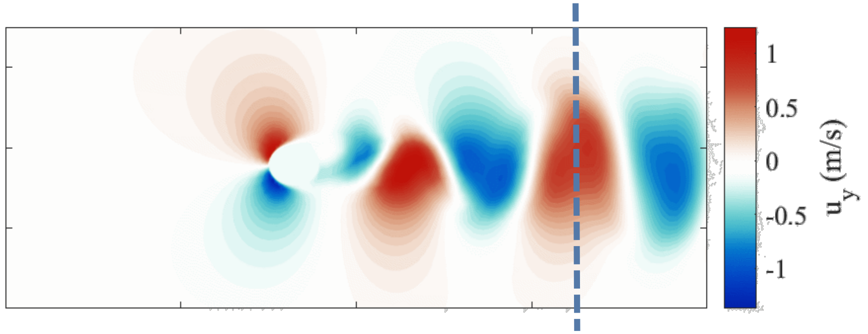

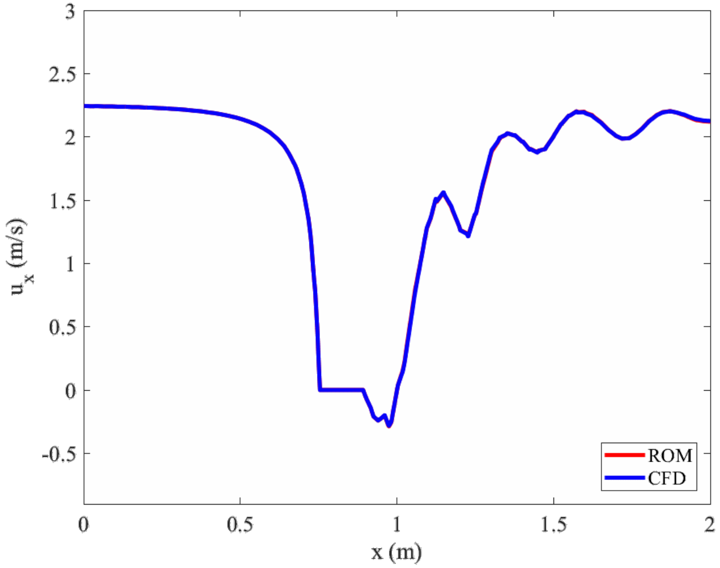

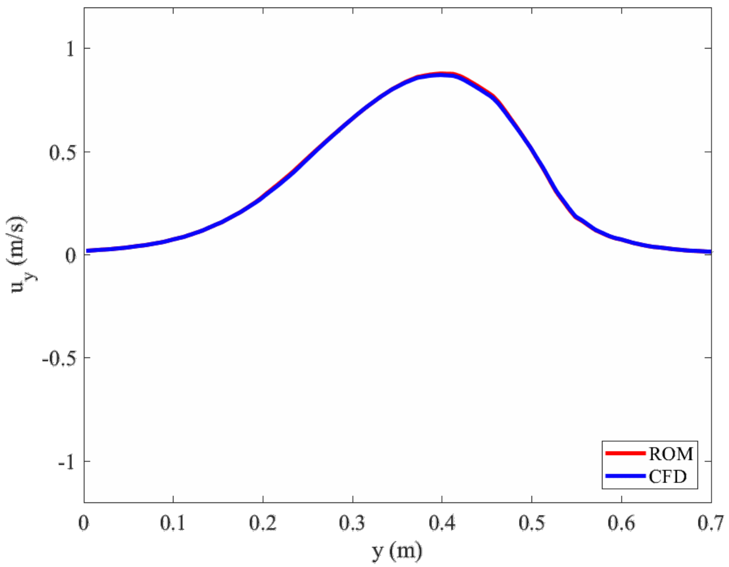

L. Gkimisis, T. Richter, P. B. (2024)

FSI: Coupled data-driven models

Fluid model:

$$\mathbf{u}_F^k = A_F \mathbf{u}_F^{k-1} + H_F \mathbf{u}_F^k \otimes \mathbf{u}_F^k + K_F\, \underline{\partial_t \mathbf{d}_F^k} \otimes \mathbf{u}_F^k + B_F\, \partial_t \mathbf{d}_s^k + L_F\, \mathbf{u}_{in}^k + C_F$$

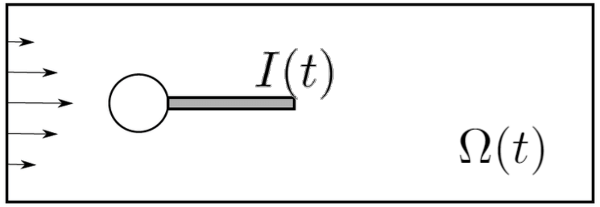

Computed from Laplace equation: $\partial_t \mathbf{d}_F^k = A_L \partial_t \mathbf{d}_s^k$

Deformable solid model:

2nd order oscillatory system: $\partial_t \mathbf{d}_s^k = A_S \underline{\partial_t \mathbf{d}_s^{k-1}} + K_S\, \underline{\mathbf{d}_s^{k-1}} + \mathbf{f}$

Forcing from the fluid stress tensor normal: $\mathbf{f} = B_S \mathbf{u}_{FS}^k + H_S \mathbf{u}_{FS}^k \otimes \mathbf{u}_{FS}^k$

Crank-Nicholson scheme for displacement update: $\mathbf{d}_s^k = \mathbf{d}_s^{k-1} + \frac{\Delta t}{2}(\partial_t \mathbf{d}_s^k + \partial_t \mathbf{d}_s^{k-1})$

Hron-Turek Benchmark FSI3

We examine the benchmark at $Re = 200$, with $t_{train} = 1.92\ s$, $t_{tot} = 3.06\ s$:

CFD data ($n = 4128$):

sFOM-POD ($r_F = 20, r_S = 5$):

L. Gkimisis, T. Richter, P. B. (2023)

Hron-Turek Benchmark FSI3

Velocity at the tip of the solid tail:

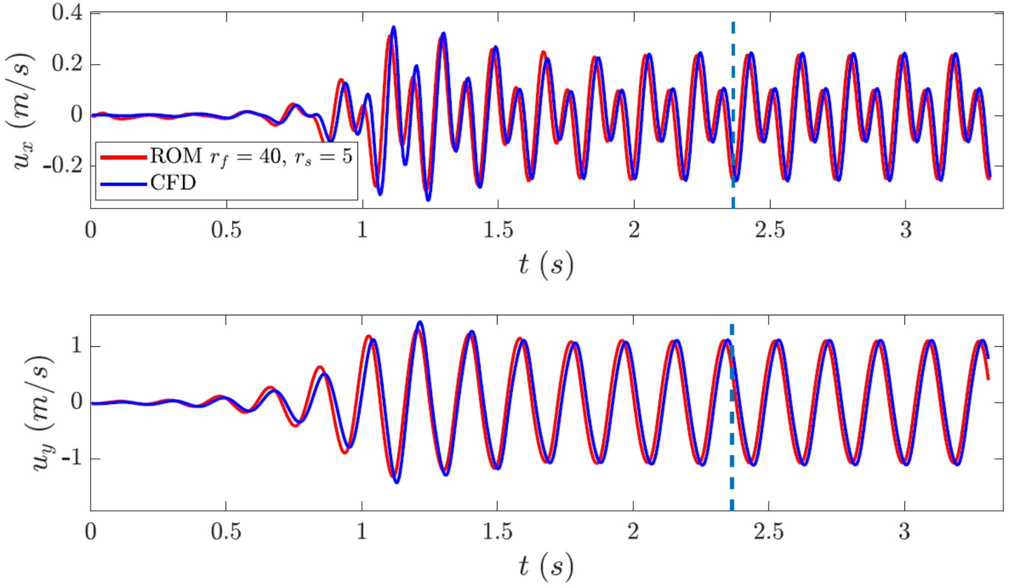

L. Gkimisis, T. Richter, P. B. (2023)

Prediction error w.r.t the POD basis dimensions r_f, r_s

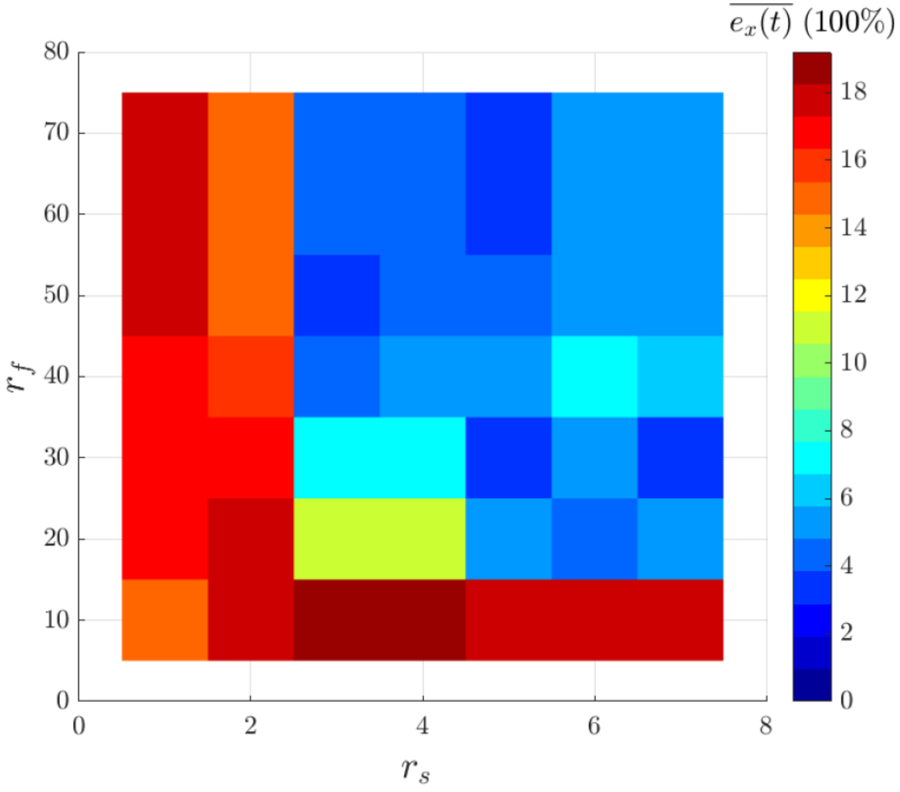

Conclusion / Future Work

So Far:

- ✓ Developed an adjacency-based method for sparse, non-intrusive modelling.
- ✓ Showcased model accuracy for 3 cases: Flow over cylinder, 2D VIV, 2D FSI.
- ✓ Investigated method properties compared to other intrusive and non-intrusive approaches.

Current / Future Work:

- Consideration of local physical constraints (e.g. energy preservation) for inferred schemes.
- Theoretical investigation of numerical scheme inference properties.
- Domain decomposition and parallelization of LS problems.
- Extension to parametric ROMs (VIV, FSI applications).

References

- Baddoo, P. J., Herrmann, B., McKeon, B. J., Nathan Kutz, J., & Brunton, S. L. (2023). Physics-informed dynamic mode decomposition. *Proceedings of the Royal Society A: Mathematical, Physical and Engineering Sciences*.

- Becker R., Braack M., Meidner D., Richter T., & Vexler B. (2002). The finite element toolkit gascoigne. https://www.gascoigne.de

- Benner P., Goyal P., Heiland J., Pones Duff I. (2021). Operator Inference and Physics-Informed Learning of Low-Dimensional Models for Incompressible Flows. *Electronic Transactions on Numerical Analysis.*

- Gkimisis, L., Richter, T., & Benner, P. (2024). Adjacency-based, non-intrusive model reduction for vortex-induced vibrations. *Computers & Fluids*.

- Gkimisis, L., Richter, T., & Benner, P. (2023). Adjacency-based, non-intrusive reduced-order modeling for fluid-structure interactions. PAMM.

- Nonino M., Ballarin F., Rozza G. (2021). A monolithic and a partitioned, reduced basis method for fluid–structure interaction problems. *Fluids.*

- Peherstorfer B., & Willcox K. (2016). Data-driven operator inference for nonintrusive projection-based model reduction. *Computer Methods in Applied Mechanics and Engineering*.

- Richter T. (2017). Coupled fluid-structure interactions. In *Lecture Notes in Computational Science and Engineering*.

- Schumann, Y., & Neumann, P. (2023). On linear models for discrete operator inference in time dependent problems. *Journal of Computational and Applied Mathematics*.

- Turek, S., & Hron, J. (2006). Proposal for numerical benchmarking of fluid-structure interaction between an elastic object and laminar incompressible flow. *Lecture Notes in Computational Science and Engineering*.